Numerical simulation and experimental study of blade pitch effect on Darrieus straight-bladed wind turbine with high solidity: A case study under realistic conditions

Milad Babadi Soultanzadeh (milad.babadi@iaukhsh.ac.ir)
Islamic Azad University Khomeini Shahr Branch https://orcid.org/0000-0003-3155-2994
Alireza Moradi
Islamic Azad University Khomeini Shahr Branch

Research

Keywords: Darrieus VAWT, Experimental aerodynamics, Computational fluid dynamics, Pitch angle, Performance coefficient

Posted Date: March 19th, 2020

DOI: https://doi.org/10.21203/rs.3.rs-17911/v1

Numerical simulation and experimental study of blade pitch effect on Darrieus straight-bladed wind turbine with high solidity: A case study under realistic conditions

Milad Babadi Soultanzadeh[1†], Alireza Moradi[2]

1† &2 Department of mechanical engineering, khomeinishahr branch, Islamic Azad University, Isfahan, Iran

†Corresponding Author Email: milad.babadi@iaukhsh.ac.ir

ABSTRACT

Numerical and experimental studies were performed to examined the influence of pitch angle on the aerodynamic performance of a small Darrieus straight blade vertical axis wind turbine with high solidity and pitch regulation system under a realistic condition. By comparing experimental and numerical results, numerical results were validated. The power coefficient was measured and calculated at different tip speed ratios and for two pitch angles 0 and 5. The results revealed that 5 degrees increase in the pitch angle led to 25% elevation in the maximum value of the power coefficient (performance coefficient). Also, the numerical results showed higher accuracy at lower tip speed ratios for both pitch angles. After numerical method validation, numerical method employed to calculate the coefficient of performance and coefficient of torque function of Azimuth position as well as the flow field in the rotor affected zone and lateral distance. According to the numerical results, vorticity generation increased by the rise in the pitch angle at a constant tip speed ratio; the maximum performance coefficient occurred at a lower tip speed ratio with elevation in the pitch angle; finally, the increment in the pitch angle led to lower velocity profile in lateral distances of the rotor.

KEYWORDS

Darrieus VAWT, Experimental aerodynamics, Computational fluid dynamics, Pitch angle, Performance coefficient

NOMENCLUTURE

A_s	rotor swept area	P	*power*
AOA	angle of attack	R	*rotor radius*

C	blades chord	T	torque
C_L	lift coefficient	TSR	tip speed ratio
C_P	power coefficient	V	velocity
C_T	torque coefficient	ρ	air density
D	rotor diameter	σ	solidity ratio
H	rotor height	ω	rotational speed
N	number of blades		

1. INTRODUCTION

Interest in renewable energy technologies has increased significantly in the recent decades given the growing chemical and thermal pollutions, rising energy demand all over the world, and depletion of fossil fuel resources. Wind has proved to be the cheapest alternative energy resource per each kWh generated electricity and has the fastest developing rate in comparison to other renewable resources such as solar energy. Two basic configurations of wind turbines are the horizontal axis wind turbines (HAWT) and vertical axis wind turbines (VAWT). The horizontal axis turbines are highly developed and used in all current large scale wind farms. On the other hand, vertical axis turbines are mostly used in urban areas and high turbulent conditions (Bhuta et al., 2012; Castelli et al., 2011). Darrieus turbines are a type of VAWTs operating through lift force in different rotor shapes and configurations (Ghasemian et al., 2017). Low start-up torque is one of the disadvantages of the Darrieus type of vertical axis turbines prompting researchers to study different geometrical parameters of Darrieus VAWT`s rotors to improve the startup performance. Numerus dimensionless parameters have been introduced in order to investigate the effect of different parameters. In recent years, many researchers have confirmed that high solidity ratio will improve the start-up torque and self-starting of Darrieus VAWTs. Otherwise, high solidity ratio has a significant negative effect on the coefficient of performance (COP) of wind turbines (Howell et al., 2009). Nevertheless, high solidity is a necessary option in low wind speed conditions. Also, different researchers have introduced blade pitch angle as a parameter which can govern VAWTs COP (Rezaeiha et al., 2017). Considerable improvements in the

understanding of VAWT can be achieved through applying CFD and experimental measurements. In this investigation, a straight blade Darrieus VAWT with high a solidity ratio has been studied numerically and experimentally under two different pitch angles in order to estimate the effect of blade pitch on the aerodynamic performance of the mentioned turbine. Many researchers have studied various aspects of VAWTs, which are briefly reviewed further.

Arab et al. (2017) examined the performance and self-starting characteristics of VAWTs numerically while considering the moment of inertia of the rotor. They used SST transient turbulent model and revealed that increase in solidity led to diminished COP average. Further, the maximum COP was calculated at lower tip speed ratios (TSR). Rezaeiha et al. (2017) applied computational fluid dynamics technique in order to study the effect of pitch angle of blades on the VAWT aerodynamics performance. They found that 6.6% increase in COP can be obtained for a certain condition of the studied turbine. Also, they demonstrated that dynamic pitching might be a very promising approach for further performance optimization. Rogowski et al. (2018) simulated a two-bladed Darrieus wind turbine using 2-D computational fluid dynamics method. They achieved good agreement between numerical and experimental results using different turbulence models such as SST k-ω and realizable k-ε. Castelli et al. (2011) proposed a new performance prediction model based on CFD. Howell et al. (2009) applied wind tunnel and numerical investigation on a small VAWT and observed that 3D numerical model had less than 20% error in comparison of wind tunnel data. Li et al. (2012) utilized 2.5-D large eddy simulation (LES) to simulate a VAWT under conditions of high angle of attack flows. Although 2.5-D LES was unable to the capture effects of the tip vortex, they solidly confirmed that 2.5-D LES is an accurate method to evaluating VAWTs aerodynamics performance. Horb et al. (2018) studied a variable pitch control for a VAWT and expressed that the variable pitch can enhance the VAWTs COP by more than 15% at the maximum power point. Danao et al. (2012) studied the effect of chamber and thickness of blades on the aerodynamics characteristic of VAWT 2-D numerically and revealed that the chamber can have a positive effect on VAWTs start-up. More relevant information is available in the literature which have been published recently (Peng et al., 2016; Sengupta et al., 2015; Svorcan et al., 2013; Nobile et al., 2014; Wang et al., 2018; Rezaeiha et al., 2018; and Sagharchi et al., 2018).

In this investigation, we intend to elucidate the effect of blades pitch angle on a specific small straight bladed Darrieus VAWT with high solidity under various tip

speed ratios (TSR) both experimentally and numerically. For this purpose, an experimental set up was assembled in Isfahan Science and Technology town, which provides desirable wind conditions and measurement instruments. Also a 2-D numerical approach was conducted to be compared against experimental results and to be validated for future studies. K-ω SST turbulent model was used to govern the full transient simulation based on dynamic mesh and six-DOF methods. The output power was measured from experimental set-up and compared with numerical results in order to dedicate accuracy of the numerical method.

2. MODEL GEOMETRY

Symmetric airfoils have been used in VAWTs in order to control the L/D ratio for downstream blades causing higher COP in comparison with chambered airfoils. While Traditionally NACA 4-digit symmetric airfoil has been selected for Darrieus straight bladed VAWTs (for example, NACA0015 to NACA0022 are widely used in various numerical and experimental studies as well as commercial applications (Ghasemian et al., 2017)). Indeed, NACA6-serie is a common airfoil family in HAWT which provides a low drag coefficient because of its top line shape. NACA630018 was employed in this regard to control the laminar boundary condition explaining the high L/D ratio. Figure.1 represents NACA630018 geometry in dimensionless coordinates.

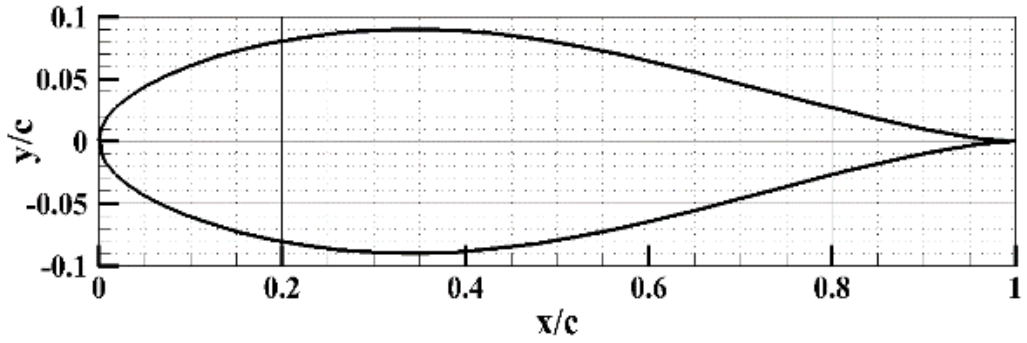

Fig. 1. NACA630018 dimensionless geometry

Another important geometrical parameter is solidity. The optimum solidity for the maximum COP has been reported within the range 0.3-0.5 (Sabaeifard et al., 2012). In this case, solidity was set 1.2. Further, other geometrical features of the studied turbine are summarized in Table 1.

Table 1. Geometrical features of the tested model

D_{rotor} [m]	0.5

H_{rotor} [m]	0.5
N [-]	3
Blade profile	NACA630018
$C_{blade\ profile}$ [cm]	10
σ [-]	1.2
Material	Wood

3.EXPERIMENTAL SET-UP

While experimental tests in wind tunnels are a very common type of tests employed to characterize VAWTs aerodynamics performance, some inaccuracies will occur because of solid blockages and wake blockages. In addition, the effect of tunnel walls is not negligible at high blockage ratios (Howell et al., 2009). Meanwhile, turbulence intensity of air stream through the test section is far smaller than under realistic conditions.

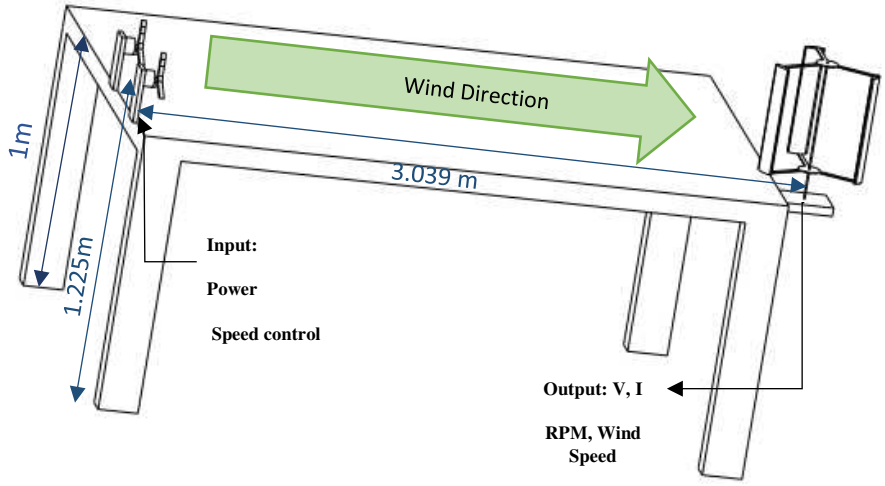

Fig. 2. Experimental setup schematic

Nevertheless, a unique experimental setup was developed in Isfahan Science and Technology Town in order to produce desirable wind conditions and to measure various parameters. Two variable speed DC motors were connected with RC speed controls to induce wind speed using two 3-bladed impellers. The impellers were installed symmetrically in relation to the turbine`s symmetrical plan. TESTO 400 was employed to measure the wind speed and rotational speed of turbine`s shaft. A servo-motor and a mechanical mechanism were applied with turbines rotor in order to apply an accurate blade pitch angle. The servo-motor could be controlled remotely. Likewise, the turbine' shaft was coupled to a low rpm DC generator; thus,

the output current and voltage were measured using an ammeter. Figure 2 illustrates the experimental setup employed in this investigation. In this case study, to generate a lower rotor moment of inertia, blades and connecting arms were manufactured using Balsa wood and employing laser cut method, see Figure 3.

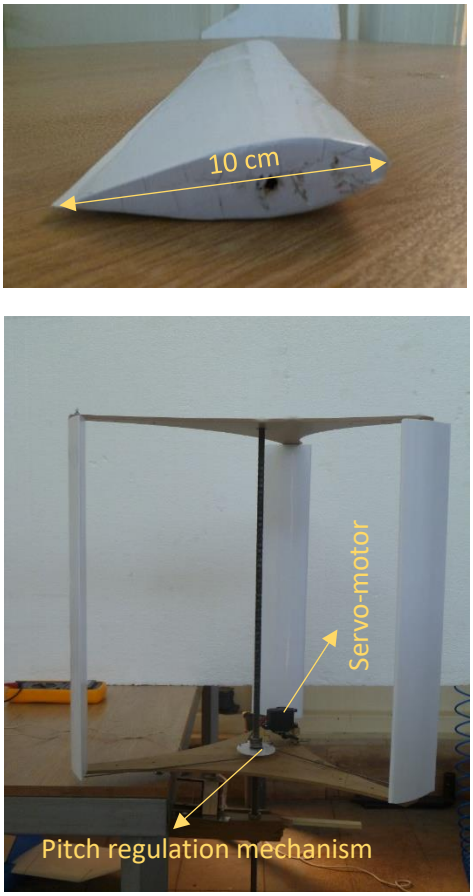

Fig. 3. Manufactured blade and tested turbine

4. NUMERICAL SETUP

Figure 4 displays the main dimensions and the boundary conditions of the whole domain Castelli et al. (2011) suggested computational domain width around 80 rotor diameter when the sides' boundary conditions are non-slip walls to establish the domain solid blockage less than 0.32%. Also, in this study all the domain boundaries were assumed velocity inlet in order to approach the realistic conditions as much as possible. Since air flow was not ducted, the domain width set 20 rotor diameter. Similarly, Li et al. (2012) set the outlet condition 12 rotor diameter after turbine to ensure full development of wake flows. An initial geometry was tested with 12 rotor diameter downstream size. The results revealed backflows on the boundaries indicating that the wake flow will not be fully developed for this case and boundary

conditions. Then, 10 rotor diameter was set for the upstream and 40 rotor diameter for the downstream after the turbine.

The numerical domain was divided into a rotational sub-grid zone simulating the revolution of the turbine by moving mesh and the main outer domain. The blades of turbines and rotational sub-grid rotated with an equal angular velocity. The turbines' blade profile in the rotational sub-grid was enclosed with an elliptic area with structured quadratic mesh and inflation of wall boundaries contributing to precise flow field solution in these areas. An unstructured triangular mesh was generated for the rest of the rotating sub-grid zone. Near-wall cell sizes were selected in a way that determined y+ less than unit on the blade profiles; thus, laminar sub-layer on the boundary layer of airfoils have been resolvable. Also, mesh independency is studied and selected grid includes124095 cells.

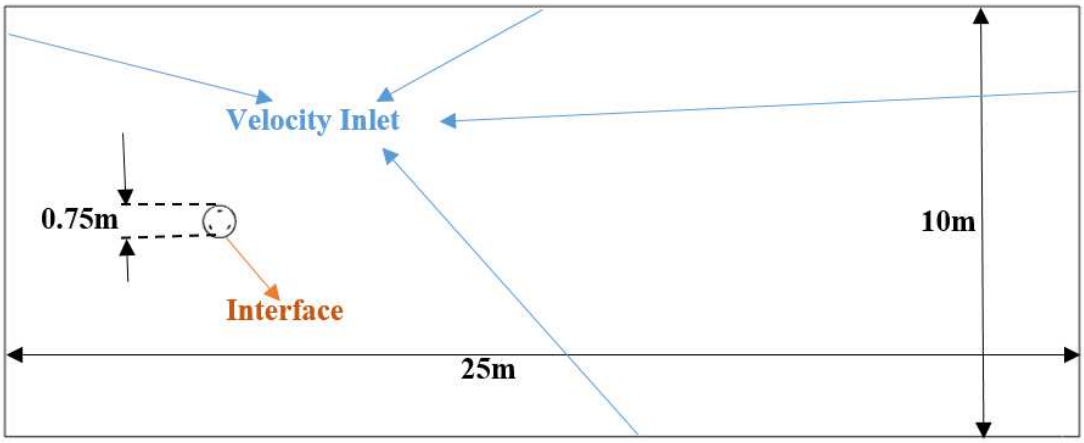

Fig. 4. Computational domain schematic and dimensions

A structured quadratic mesh with refinement near the rotational zone was applied to the domain. Also, the wake line back of the turbine rotor was meshed finely where the vortex cores were able interact completely thereby enhancing the calculation accuracy in the wake flow. The interface between the rotating zone and the main outer domain was a non-conformal interface with coupled grid to allow the turbine rotation. Figure 5 presents detailed generated meshes in different zones.

The incompressible momentum equation and continuity are appropriate for solving VAWT flow field, as the induced velocities are smaller than Mach number 0.3 (Li et al., 2012). Various turbulence models have been employed and comprised by previous researchers with both RANS and eddy simulations (LES and DES) being validated with different experimental tests (Sanderse et al., 2011). Because of the

unsteady nature of wind turbines flow field, 3-D LES has shown the most acceptable results, but the computational cost is extremely high for this method. Meanwhile, 4-equation SST turbulence model was used by Rezaeiha et al. (2017) which yielded a good agreement with experimental data. In this study, the incompressible 2-D transient RANS equations were solved using coupled pressure-velocity scheme with 6-DOF dynamic mesh option being selected. The 4-equation Transition SST with DES scale-resolving simulation option were employed as a turbulence model.

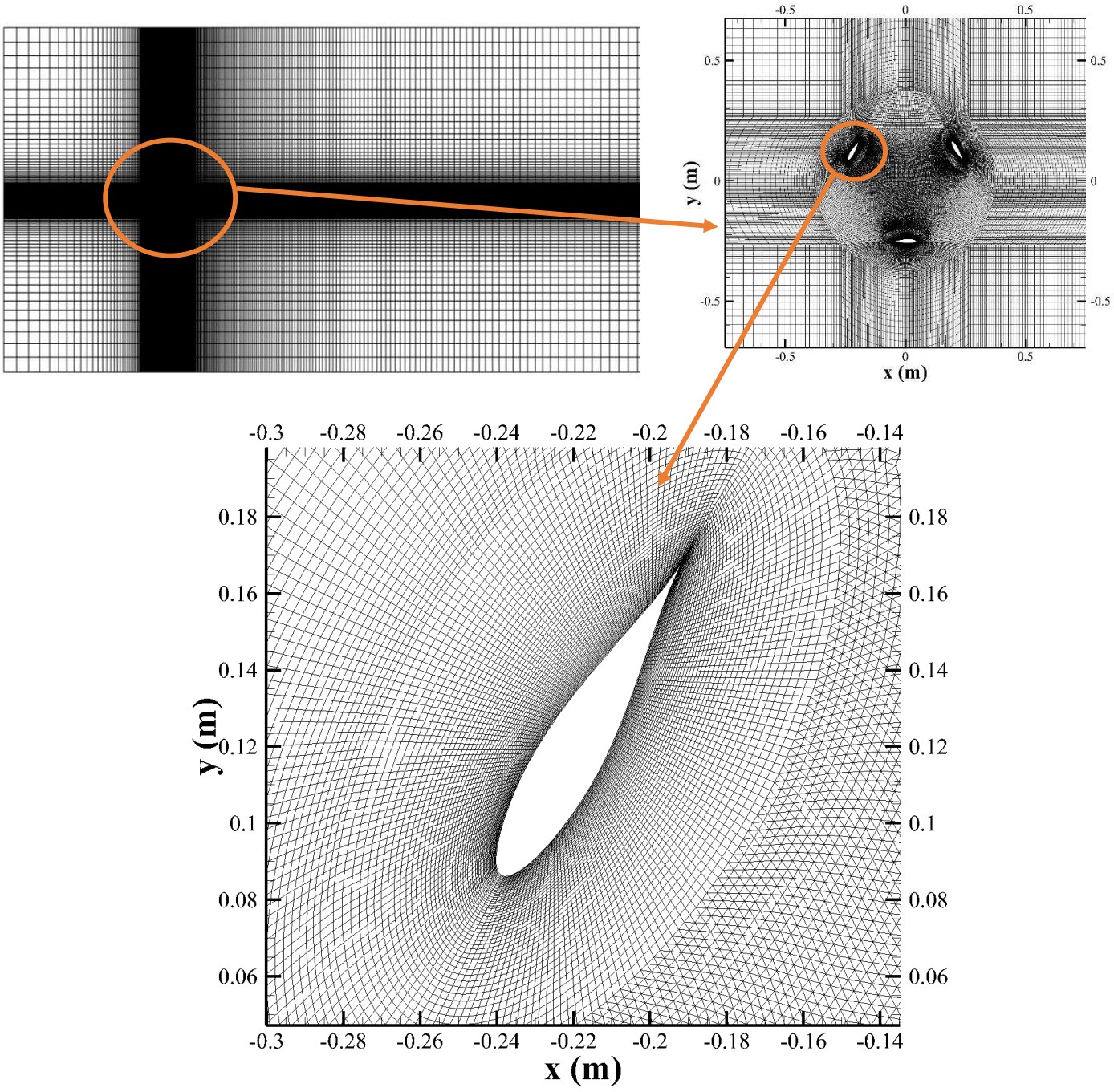

Fig. 5. Detailed generated mesh for numerical domain

The initial solution was based on steady state RANS and K-ε turbulence model. Then, a specific time step for each TSR was set such that the turbine rotated 2 degrees per each time step. Converging criteria were set to 10-4 for all absolute residuals. Data were extract after five complete rotations of the turbine revealing convergence in the torque-time diagram.

regarding to $\frac{\delta}{x} = 0.385{R_e}^{-0.2}$ the boundary layer thickness is 5.65cm. The distance between table and bottom surface of rotor is 3.2cm. According to (Orgaz et al. 2011 and Narayan 1977), at $\frac{\delta}{y} \geq 0.6$ velocity profile is approximately smooth. Also, only 4.9% of blade length is affected by this smooth area of boundary layer which is negligible.

5. RESULTS AND DISCUSSION

There are various methods for the initial design and evaluation of VAWTs. Since all of them require the aerodynamics characteristic of blade profiles (Carrigan et al., 2011; Ghasemian et al., 2017), an initial simulation was applied to NACA630018 airfoil employing viscous panel method and computational fluid dynamics to estimate the lift and drag coefficient at various angles of attack. XFOIL open-source code was used to apply the viscous panel method with the results being comprised with 2-D CFD steady state simulation in Figure6.

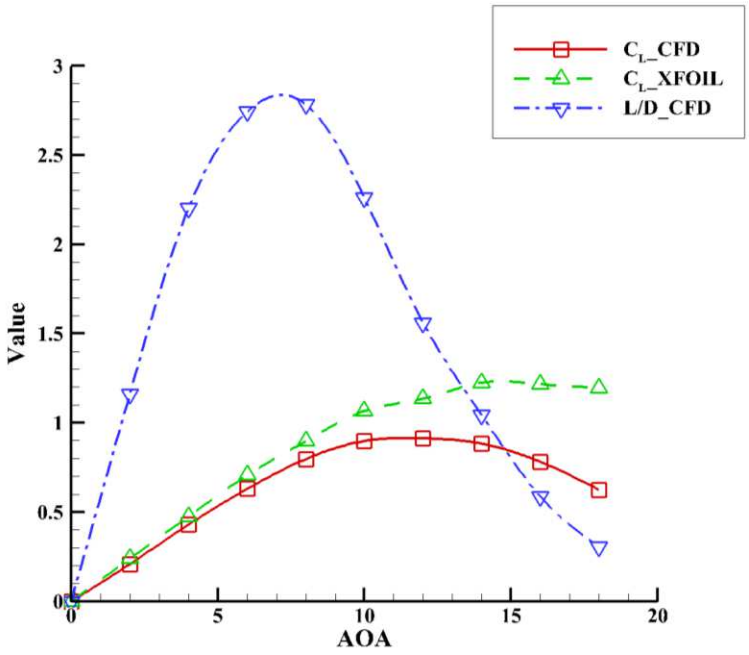

Fig. 6. Aerodynamic characteristics of NACA630018

According to Figure 6, the viscous panel method and CFD have a good agreement at low angles of attack; however, as the boundary layer separation begins, at higher angles of attacks CFD shows more accurate aerodynamics load coefficients. L/D ratio increased in AOAs less than 7 degree and diminished thereafter such that the maximum L/D ratio occurred near 7-degree AOA for NACA630018.

Figure 7 depicts the averaged COP evolution calculated and measured employing CFD and experimental tests for various tip speeds. The COP and Tip speed ratio (TSR) are represented as below (Castelli et al., 2011):

$$C_P = \frac{P_{ave}}{\frac{1}{2}\rho A_s V_{wind}^{3}} \quad (1)$$

$$TSR = \frac{\omega R_{Rotor}}{V_{wind}} \quad (2)$$

Figure 7 illustrates that the maximum COP for the pitch angle 5° is 25.41671% higher than the maximum COP for the pitch angle 0° with the maximum COP occurring at lower TSRs with increase in the pitch angle, since the blades' relative angles of attack diminish when transitioning from lower to higher TSR values. Also, CFD results indicated higher accuracy at lower TSRs. Further, positive COP occurred at low tip speeds because of high solidity. Solidity is one of the main dimensionless ratios dictating the rotational velocity at which the turbine reaches its maximum COP. Note that higher solidity leads to lower tip-speed ratios and lower efficiency (Howell et al., 2009).

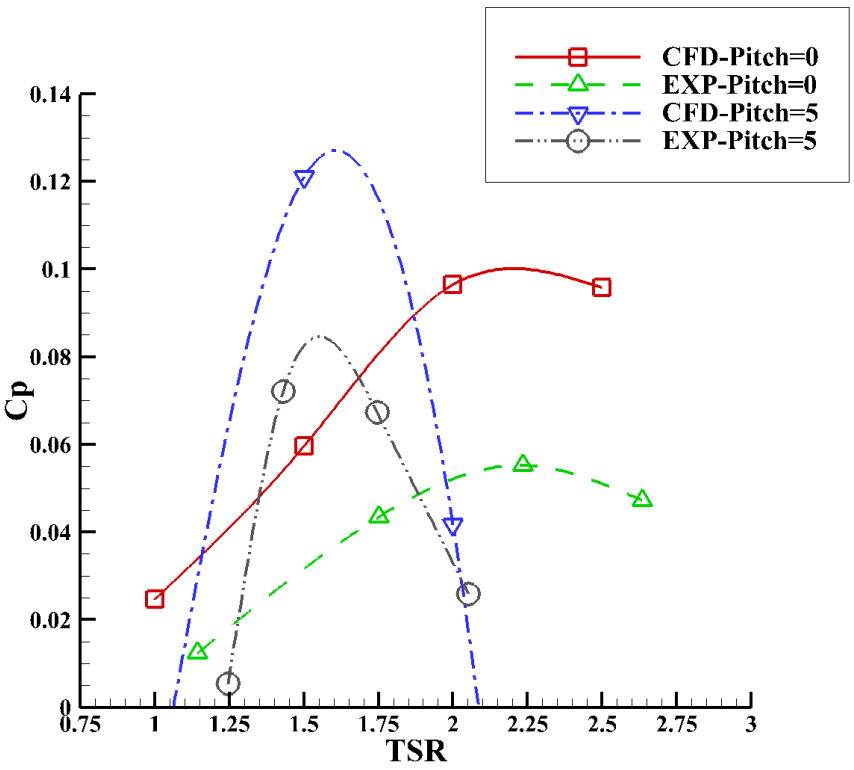

Fig. 7. Coefficient of performance in various tip speed ratios

Solidity is defined as Equation (3) (Rezaeiha et al., 2017):

$$\sigma = \frac{N_{blade} C_{blade}}{R_{rotor}} \tag{3}$$

The pitch angle has found to have significant influence for power generated of the turbine. However, the optimum fixed pitch angle should be calculated such that the maximum value of performance and positive region of CP as well as highest start-up torque are taken into account.

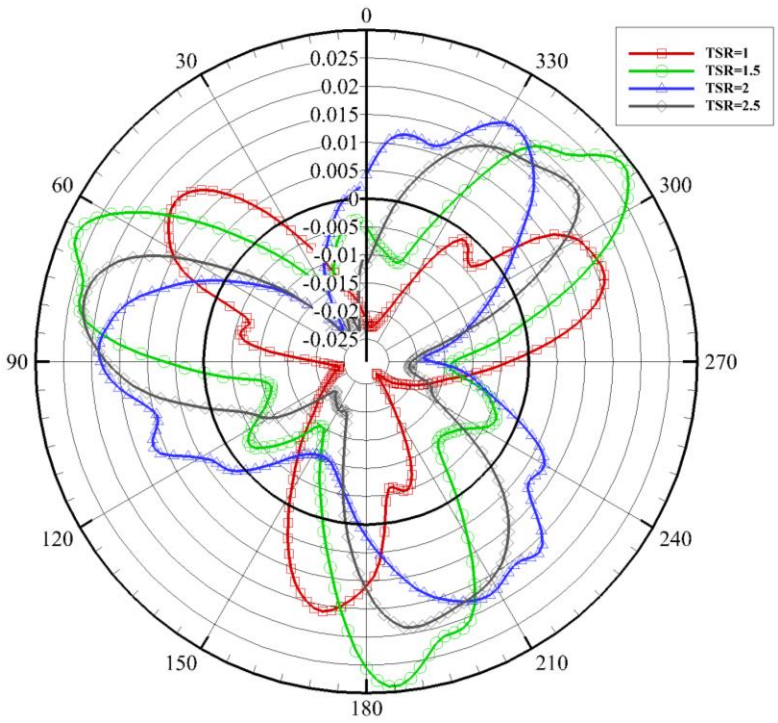

Fig. 8. Evolution of CT as function of Azimuth position for TSR=1, 1.5, 2, 2.5; respectively in pitch=0.

Comparison of the numerical simulations with experimental measurements revealed that numerical prediction using Transition SST with DES scaled-resolving turbulence model is able to replicate the shape and curve of experimental data as well as accuracy in capturing the maximum power coefficient tip speed ratio. The discrepancies between experimental and numerical results caused by different 2-D inabilities. For instance, tip losses are neglected in 2-D simulations as well as upper and bottom rotor arms effects on moment of inertia and drag force of rotor. Also, rotor arms will produce turbulent vortices which effect the aerodynamic performance of downstream blades (Castelli et al. 2011).

Figure 8 illustrates the evolution of the coefficient of torque for TSR=1, 1.5, 2, 2.5 at a zero pitch angle. With the rotational speed being constant for each single TSR, Figure 8 represents a schematic view of COP evolution function of Azimuth angle. Based on Figure 8, the highest averaged CT occurred at TSR=1.5. Further, the positive area of CT was maximum for TSR=1.5, while TSR=1 showed the minimum area of CT. The coefficient of torque is defined as Equation (4):

$$C_T = \frac{T_{rotor}}{\frac{1}{2}\rho A_s R_{rotor} V_{wind}^2} \tag{4}$$

The areas with negative CT developed as the blades travelled into the dynamic stall condition causing diminished L/D ratio. Dynamic stall occurred due to high angle of attack through the blades' revolution and influence of shed wakes of the upwind blades on the downstream blades.

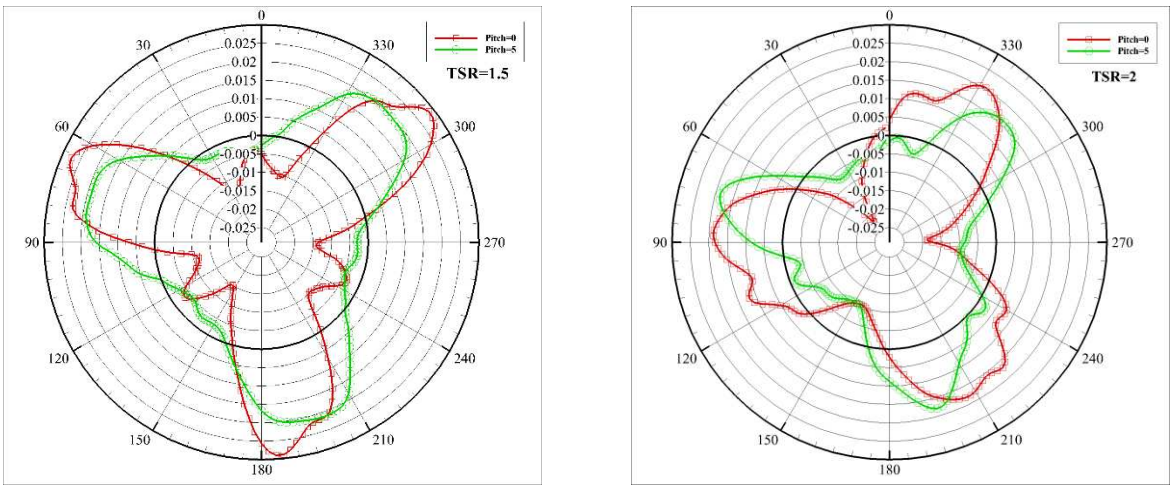

Fig. 9. Evolution of CT as function of Azimuth position for pitch angle 0 (red) and 5(green) in TSR=1.5 and 2 respectively.

Figure 9 presents comparative diagrams of CT at TSR=1.5 and 2 for pitch angle 0^{o} and 5^{o} respectively. According to Figure 9 for TSR=1.5, the average and positive area of CT at pitch=5 is higher than that at pitch=0 causing a higher COP in Figure 7. An increase in the pitch angle led to elevated angle of attack in the downstream blades condition and augmented the L/D ratio in these areas. Also, the diagram of CT at TSR=1.5 for pitch=5 has a smoother peak in comparison to pitch=0 due to delayed dynamic stall. On the other hand, at TSR=2, most of the area for pitch=5 diagram is negative suggesting more low angle of attack in the revolution of blades.

Figure 10 illustrates CT for a single blade function of Azimuth position at TSR=1.5 for pitch=0 and 5. According to Figure 10, the average torque coefficient for a single blade with pitch=5 is higher than the same blade with pitch=0 at TSR=1.5. While TSR is constant, the influence of shed wakes is equal for both pitch conditions. It means there is an influence of angle of attack on the torque coefficient. Note that the blades at TSR=1.5 experienced the optimum angle of attack with pitch angle 5.

Instantaneous vorticity magnitude for three Azimuth positions are presented in Figure 11. Since it is a 2D simulation, according to the incompressible vorticity transport equation, the vorticity is generated from the wall and diffused through fluid viscosity in the x-y plane (Li et al., 2012).

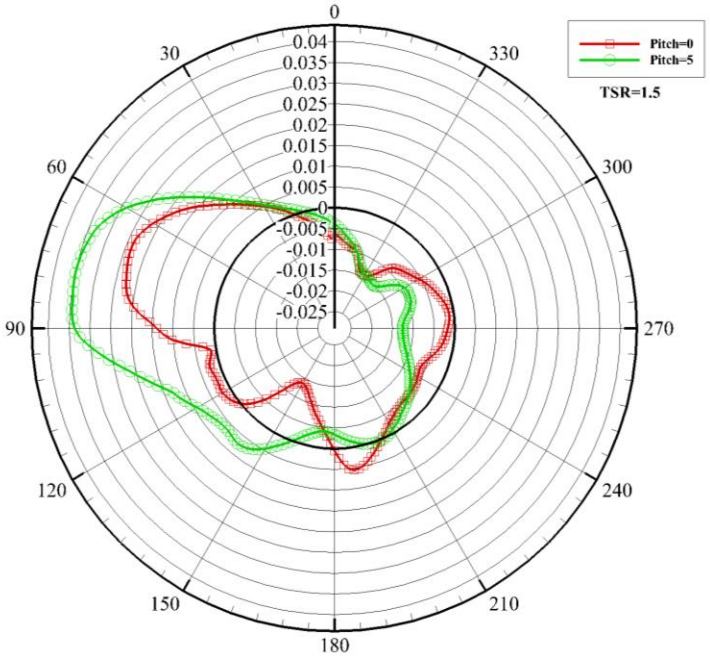

Fig. 10. Evolution of CT as function of Azimuth position for a single blade at TSR=1.5; pitch=0(red) and pitch=5(green)

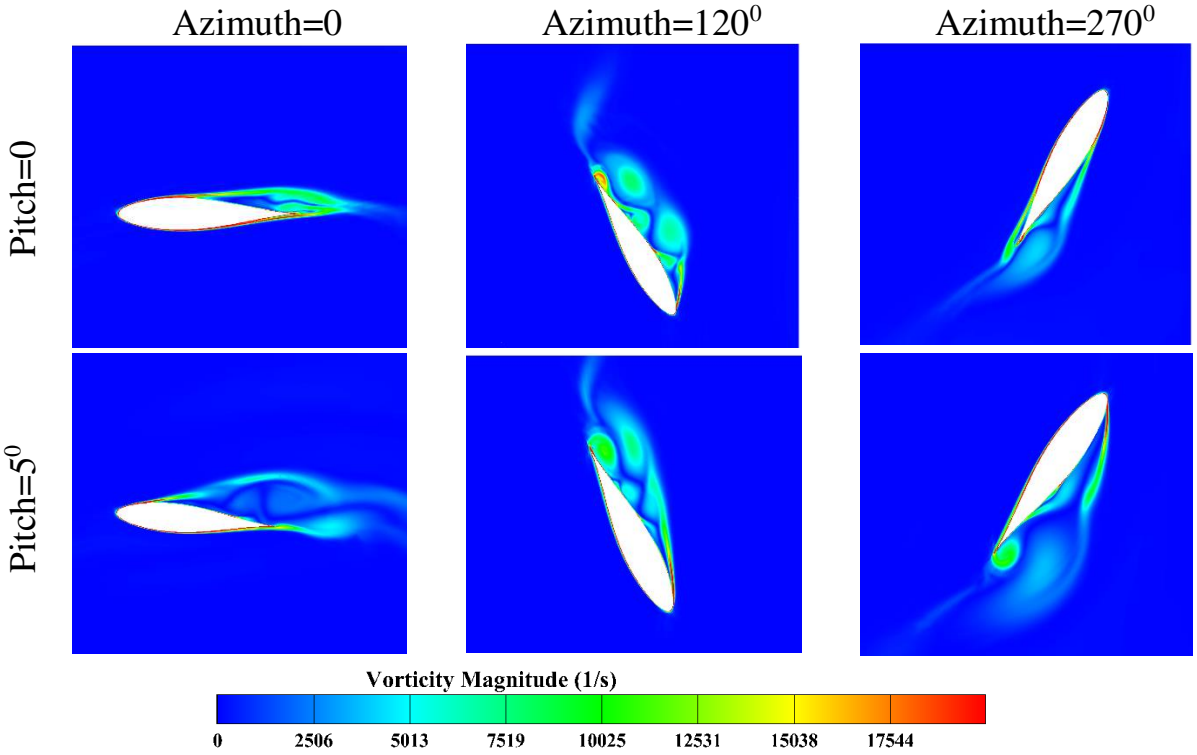

Fig. 11. Vorticity magnitude (1/s); TSR=2

Based on Figure 11, high vorticity distribution zones are wider for pitch=5. An increase in the pitch angle led to more interactions between the sloid wall and

viscous flow, widening high vorticity zones. Note that the shape of the vorticity distribution at both pitch angles is similar, but the distribution of high vorticity region is wider for pitch 5.

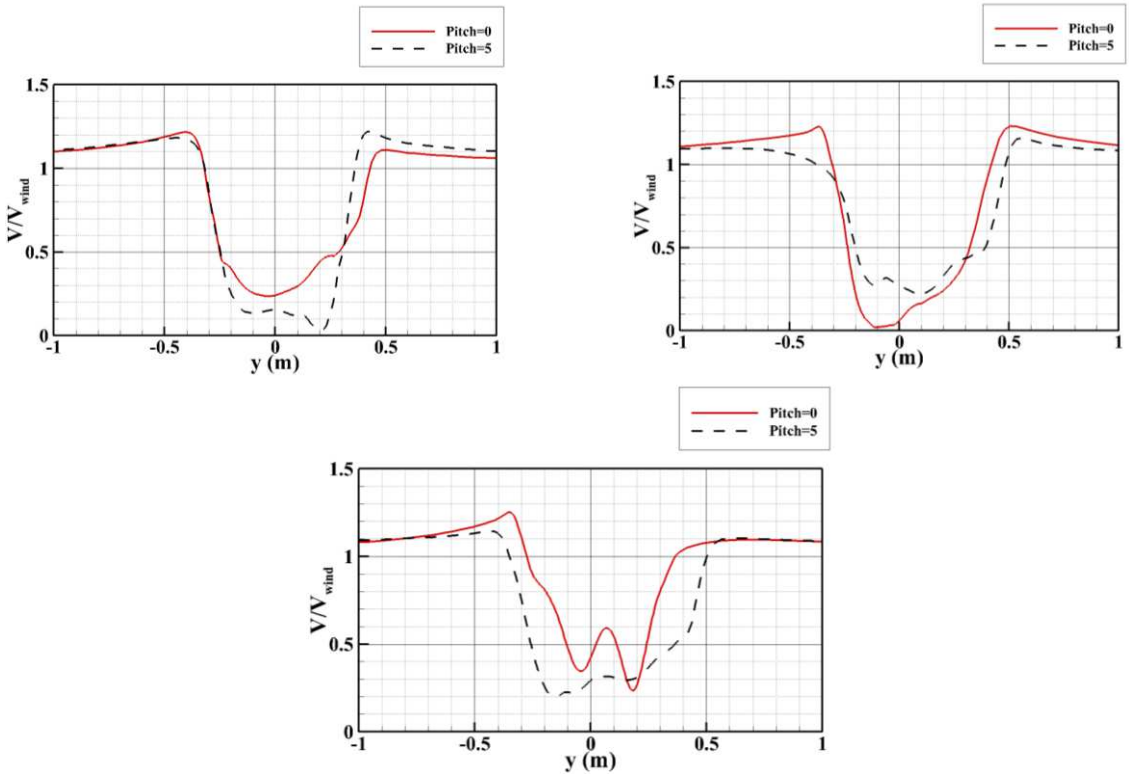

Fig. 12. Cross stream dimensionless velocity profile in 1D, 2D and 3D lateral distance of turbine (CFD results)

Since wake characteristics have a significant impact on the aerodynamic design of single turbines and the optimal placement of wind-farms (Peng et al., 2015), dimensionless stream velocity in 1, 2, and 3 times of the rotor diameter were calculated and represented in Figure 12 at TSR=2 for both 0 and 5 pitch angles. This parameter was calculated after 20 revolutions of the turbine when the wake development was completed in reference of Azimuth position. According to Figure 12, the averaged velocities for pitch=5 are lower than same parameter for pitch=0 at 1D and 3D lateral distance. Conversely, the averaged velocity for pitch=5 is higher than the same parameter for pitch=0 at 2D lateral distance. The turbine wake developed from the generated vortices shed of blades while revolving (Rezaeiha et al., 2018). Vortices travel to downstream and make changes in the velocity profile behind the turbine. The changes in the magnitude of vortex are a function of

variations in the angle of attack. The wider region of vorticities in pitch=5 leads to a greater influence on the velocity profile in lateral distances.

6. CONCLUSION

A small straight bladed VAWT with high solidity ratio was manufactured and tested under realistic conditions. Further, supportive numerical simulations were conducted to evaluate the aerodynamic performance of the turbine at various tip speed ratios and two pitch angles 0 and 5, in order to examine the influence of the pitch angle on the aerodynamic characterization of the turbine. The results revealed that increase in the pitch angle caused elevated maximum COP while making the CP_TSR diagram sharper. The maximum CT occurred at TSR for turbines without pitch angle, but the maximum CP occurred at TSR=2. The averaged CT increased upon elevation of the pitch angle at TSR=1.5, though diminished at TSR=2. Single blade CT increased with the rise in the pitch angle at TSR=1.5. Likewise, the vorticity generation increased due to elevation of the pitch angle causing increased angle of attack. Finally, the increase in the pitch angle led to a greater influence on the velocity profile in the lateral distance of turbine and generated lower velocity wakes.

Acknowledgments

The authors would like to thank the Isfahan Science and Technology Town (ISTT) for their supports.

Authors` Contributions

Corresponding author has applied numerical simulations and second author has been working on prototyping and experimental set up. All the numerical results and measured data have been collected by corresponding author. All authors have read and approved final manuscript.

Funding

Isfahan Science and Technology Town has granted a loan base on our business plan to develop an urban vertical axis wind turbine.

Availability of Data and Materials

Parts of the data and materials are available upon request.

Competing interests

The authors declare that they have no competing interests.

REFERENCES

Bhuta, M. M. A. et al (2012). Vertical axis wind turbine- A review of configurations and design techniques. Renewable and sustainable energy reviews 16, 1926-1939.

Casteli, M. R. (2011). The Darrieus wind turbine: proposal for a new performance prediction model based on CFD. Energy 36, 4919-4934.

Ghasemian, M. et al (2017). A review on computational fluid dynamic simulation techniques for Darrieus vertical axis wind turbines. Energy conversion and management 149, 87-100.

Howell, R. et al (2009). Wind tunnel and numerical study of a small vertical axis wind turbine. Renewable energy 35, 412-422.

Rezaieha, A. et al (2017). Effect of pitch angle on power performance and aerodynamics of a vertical axis wind turbine. Applied energy 197, 132-150.

Arab, A. et al (2017). A numerical study on the aerodynamic performance and self-starting characteristics of a Darrieus wind turbine considering its moment of inertia. Renewable energy, Article in press.

Rogowski, K. et al (2018). 2-D computations of the two-bladed Darrieus-type wind turbine. Journal of applied fluid mechanics 11(4), 835-845.

Li, C. et al (2012). 2.5D large eddy simulation of vertical axis wind turbine in consideration of high angle of attack flow. Renewable energy 51, 317-330.

Horb, S. et al (2018). Variable pitch control for vertical-axis wind turbine. Wind engineering 42(2), 128-135.

Danao, L. A. et al (2012). A numerical study of blade thickness and camber effects on vertical axis wind turbines. Journal of power and energy 226(7), 867-881.

Peng, H. Y. et al (2015). Investigation into the wake aerodynamics of five-straight-bladed vertical axis wind turbine by wind tunnel test. Journal of wind engineering and industrial aerodynamics 155, 23-35.

Sengupta, A. R. et al (2016). Studies of some high solidity symmetrical and unsymmetrical blade H-Darrieus rotors and flow physics in low wind stream. Renewable energy 93, 536-547.

Svorcan, J. et al. (2013). Aerodynamic design and analysis of a small-scale vertical axis wind turbine. Journal of mechanical engineering and technology 27(8), 2367-2373.

Nobile, R. et al. (2011). Dynamics stall for a vertical axis wind turbine in two-dimensional study. World renewable energy congress, may 2011 Linkoping, Sweden.

Wang, Y. et al. (2018). Investigation on aerodynamic and performance of vertical axis wind turbine with different series airfoil shapes. Renewable energy 126, 801-818.

Rezaeiha, A. et al. (2018). Characterization of aerodynamic performance of vertical axis wind turbines: Impact of operational parameters. Energy conversion and management 169, 45-77.

Sagharichi, A. et al. (2018). Effect of solidity on performance of variable-pitch vertical axis wind turbine. Energy, Article in press.

Sabaeifard, P. (2012). A determination of vertical axis wind turbines optimal configuration through CFD simulations. International conference of future environment and energy (2012) 28, 109-13.

Sanders, B. et al. (2011). Review of computational fluid dynamics for turbine wake aerodynamics. Wind energy 14, 799-819.

Carrigan, T. J. et al. (2012). Aerodynamics shape optimization of a vertical-axis wind turbine using differential evolution. ISRN Renewable energy 2012, 16 pages.

P. A. Aswatha Narayana (1977). Turbulent boundary layer velocity profile over smooth surface. Applied Scientific Research 33. Springer 1977, 427-435.

391 Orgaz et al. (2011). Power-law velocity profile in turbulent boundary layers: An
392 integral Reynolds-number dependent solution. Acta Geophysica 59. 933-1012.

Figures

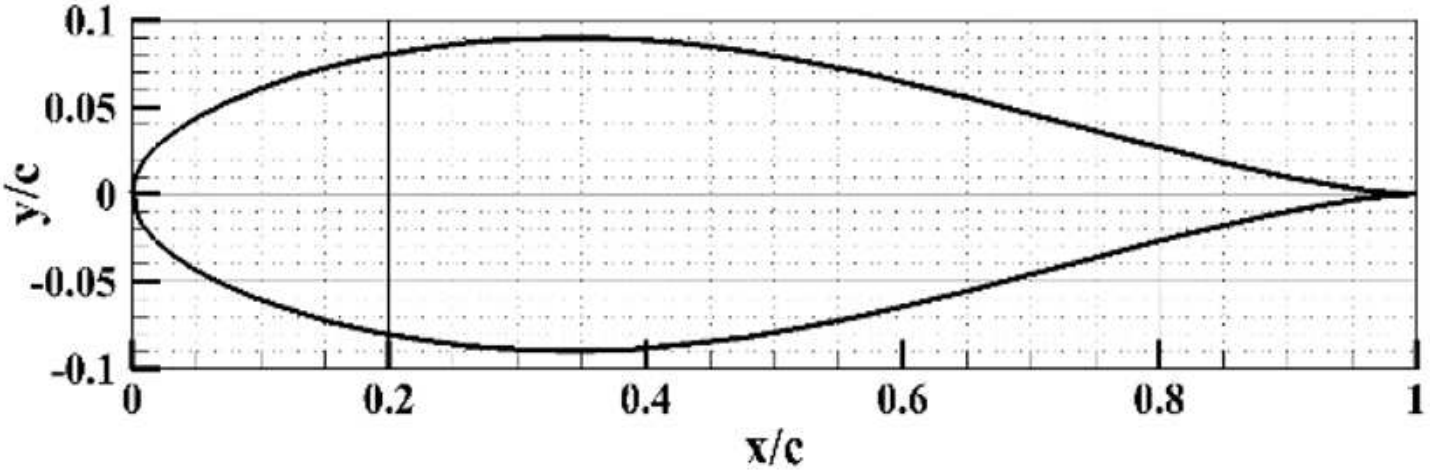

Figure 1

NACA630018 dimensionless geometry

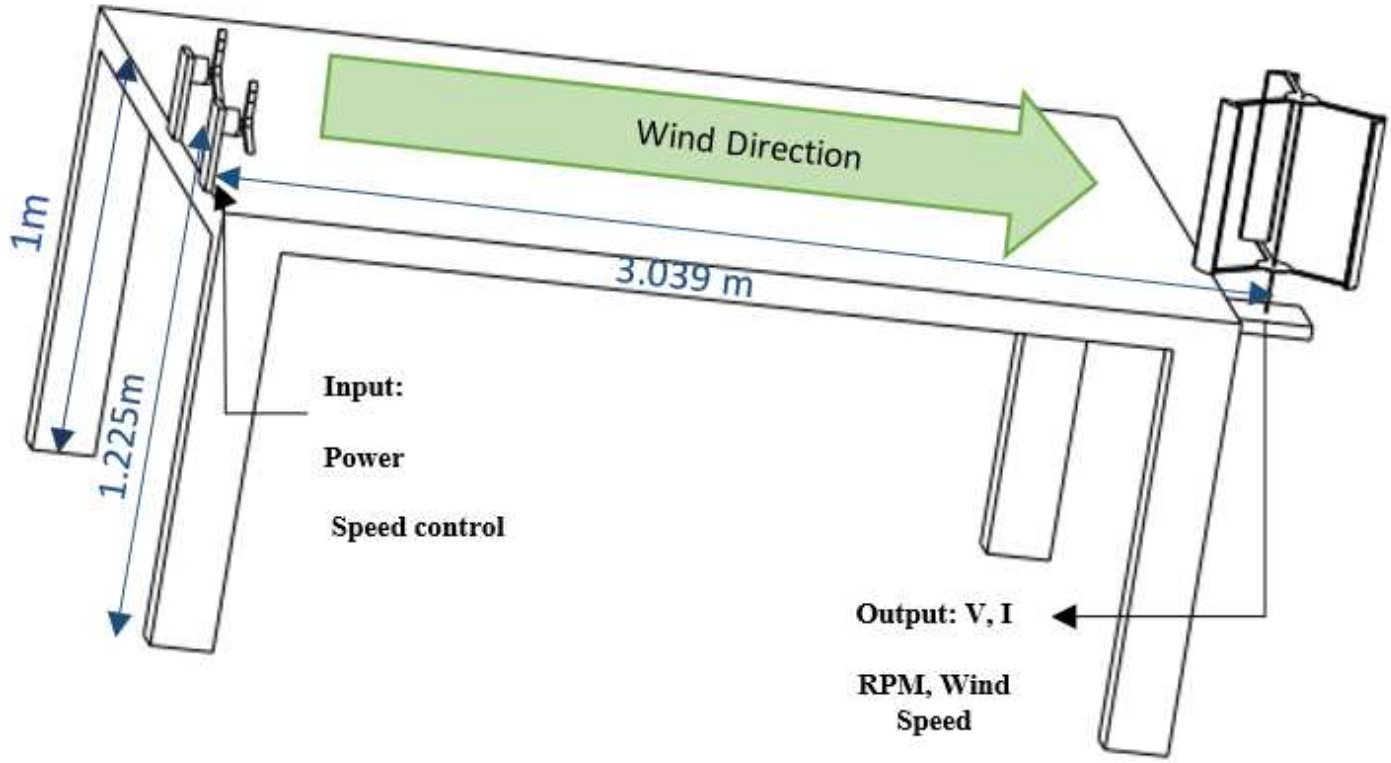

Figure 2

Experimental setup schematic

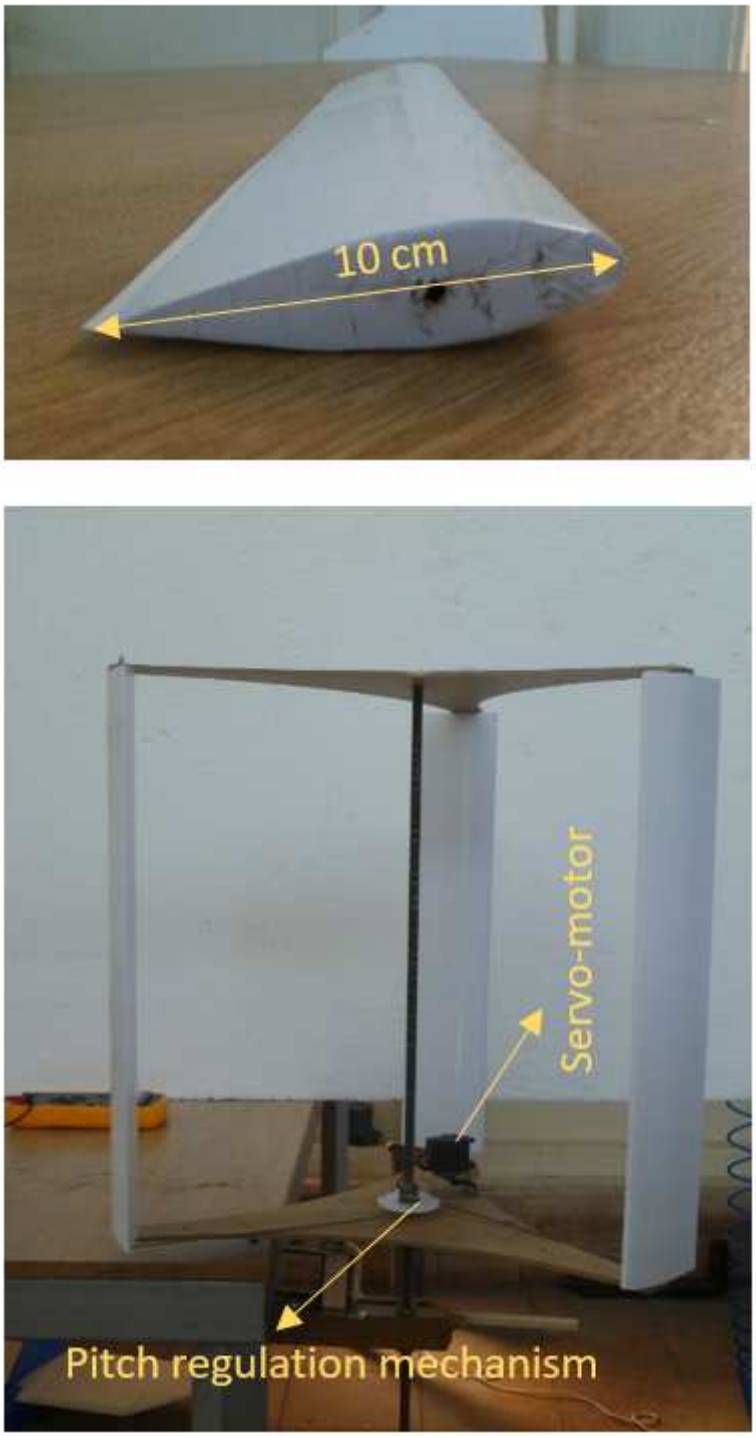

Figure 3

Manufactured blade and tested turbine

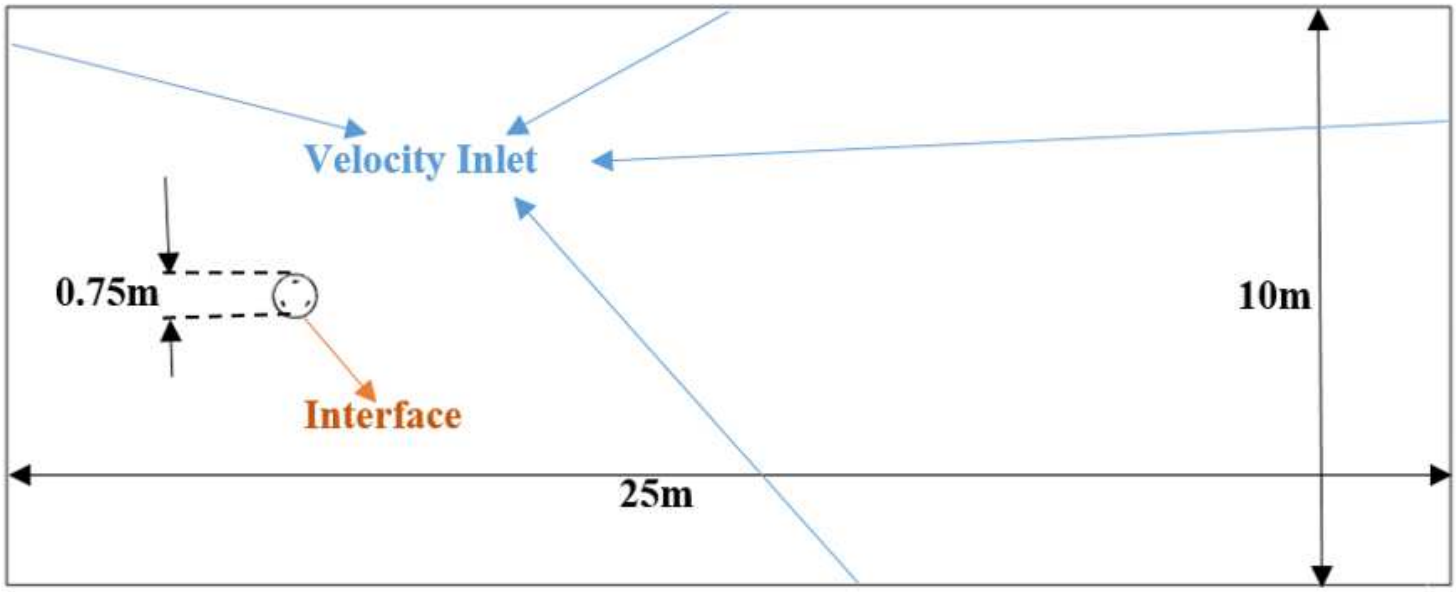

Figure 4

Computational domain schematic and dimensions

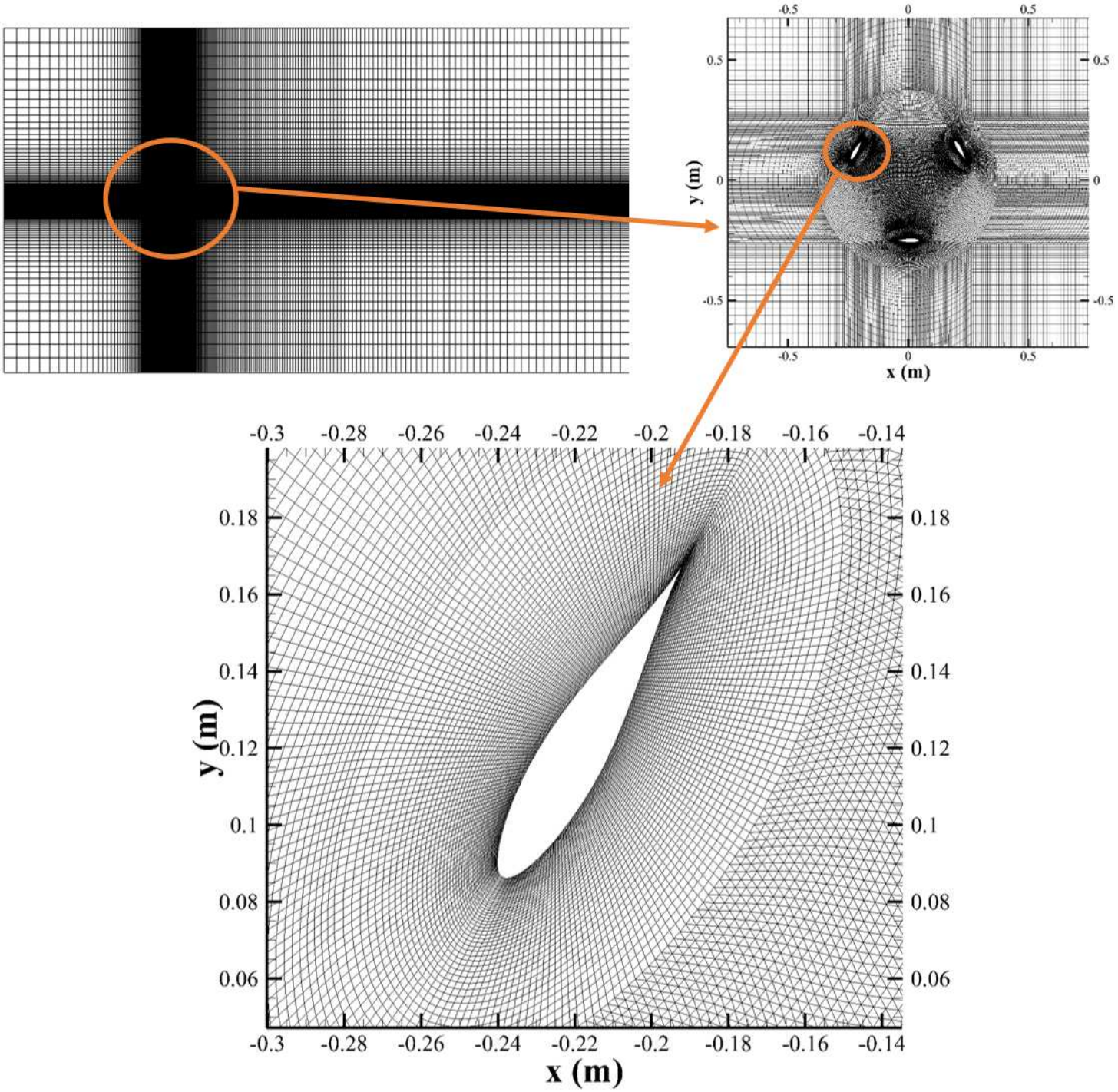

Figure 5

Detailed generated mesh for numerical domain

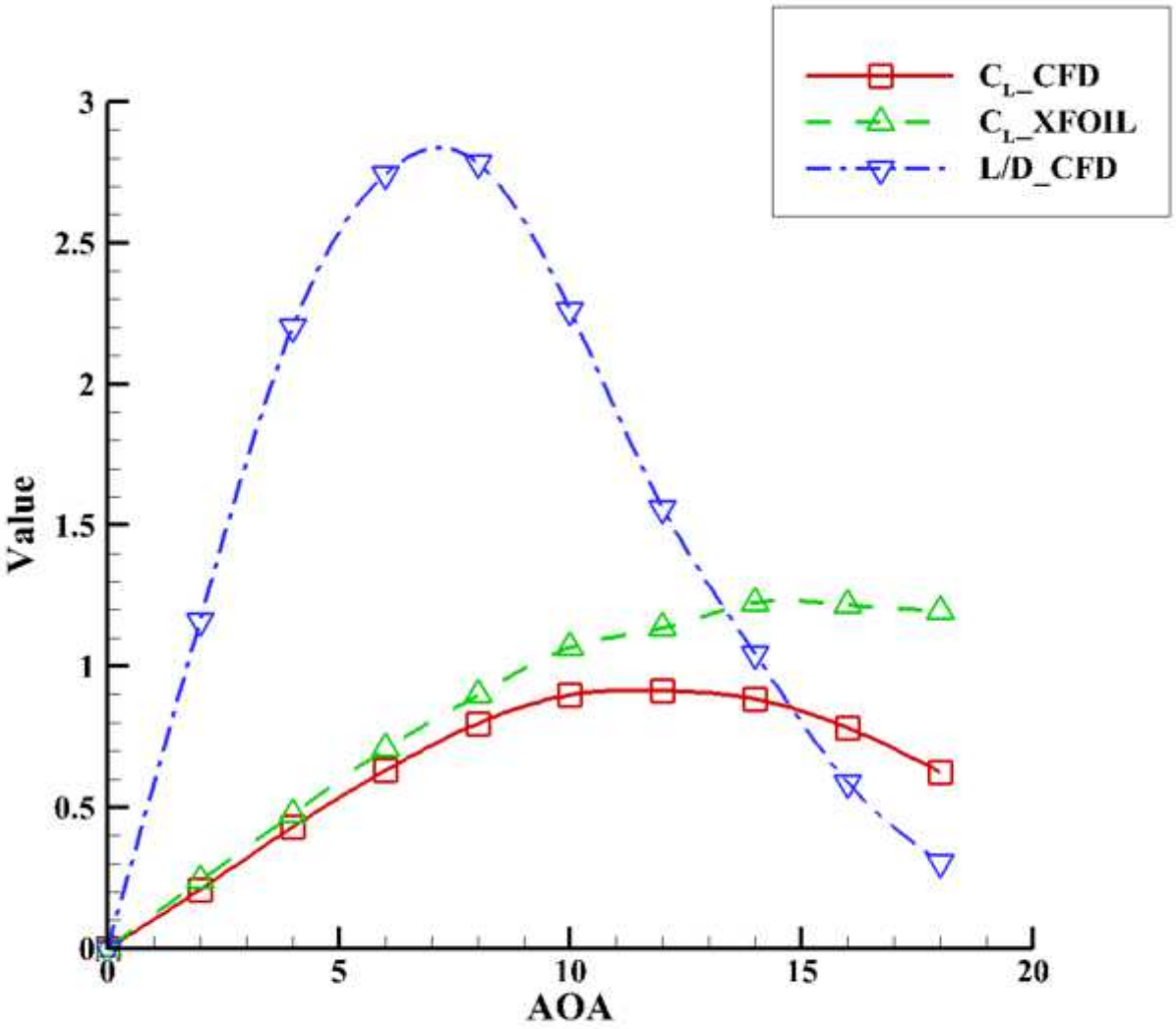

Figure 6

Aerodynamic characteristics of NACA630018

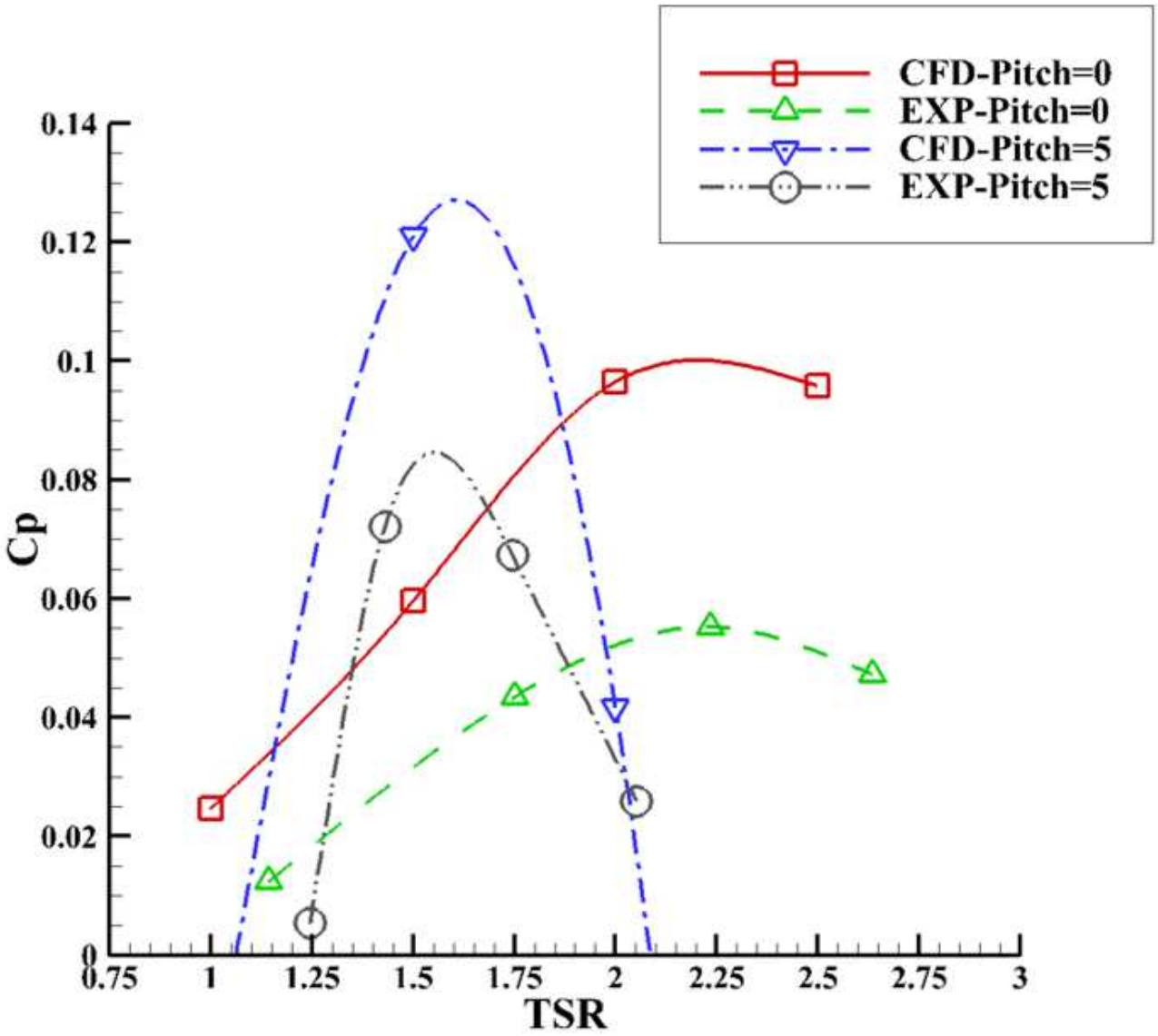

Figure 7

Coefficient of performance in various tip speed ratios

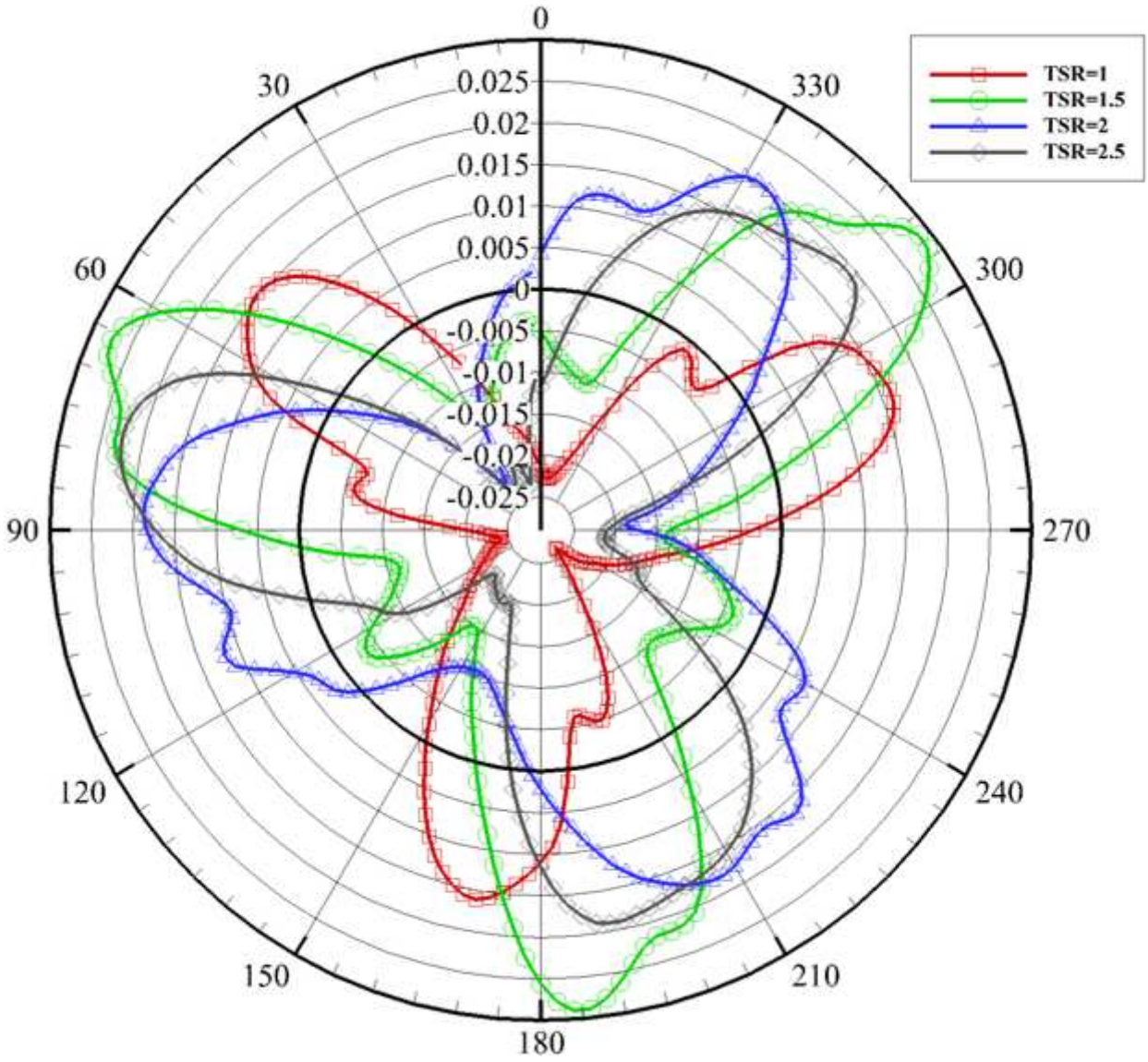

Figure 8

Evolution of CT as function of Azimuth position for TSR=1, 1.5, 2, 2.5; respectively in pitch=0

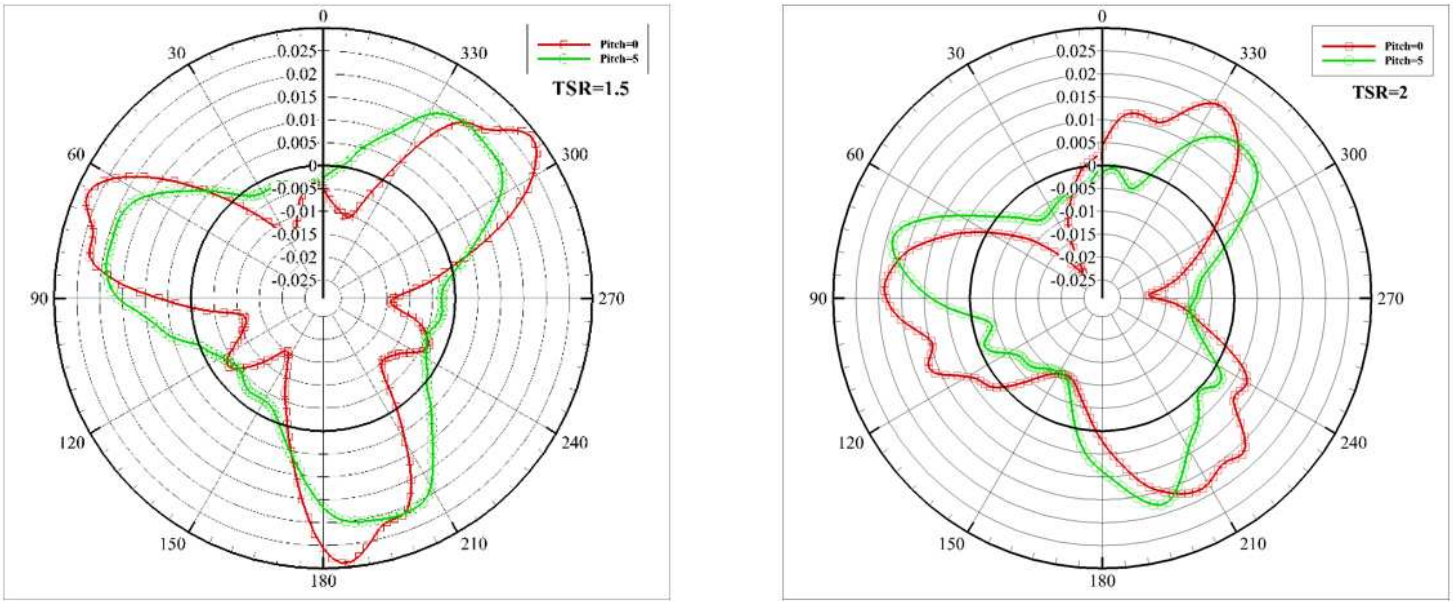

Figure 9

Evolution of CT as function of Azimuth position for pitch angle 0 (red) and 5(green) in TSR=1.5 and 2 respectively.

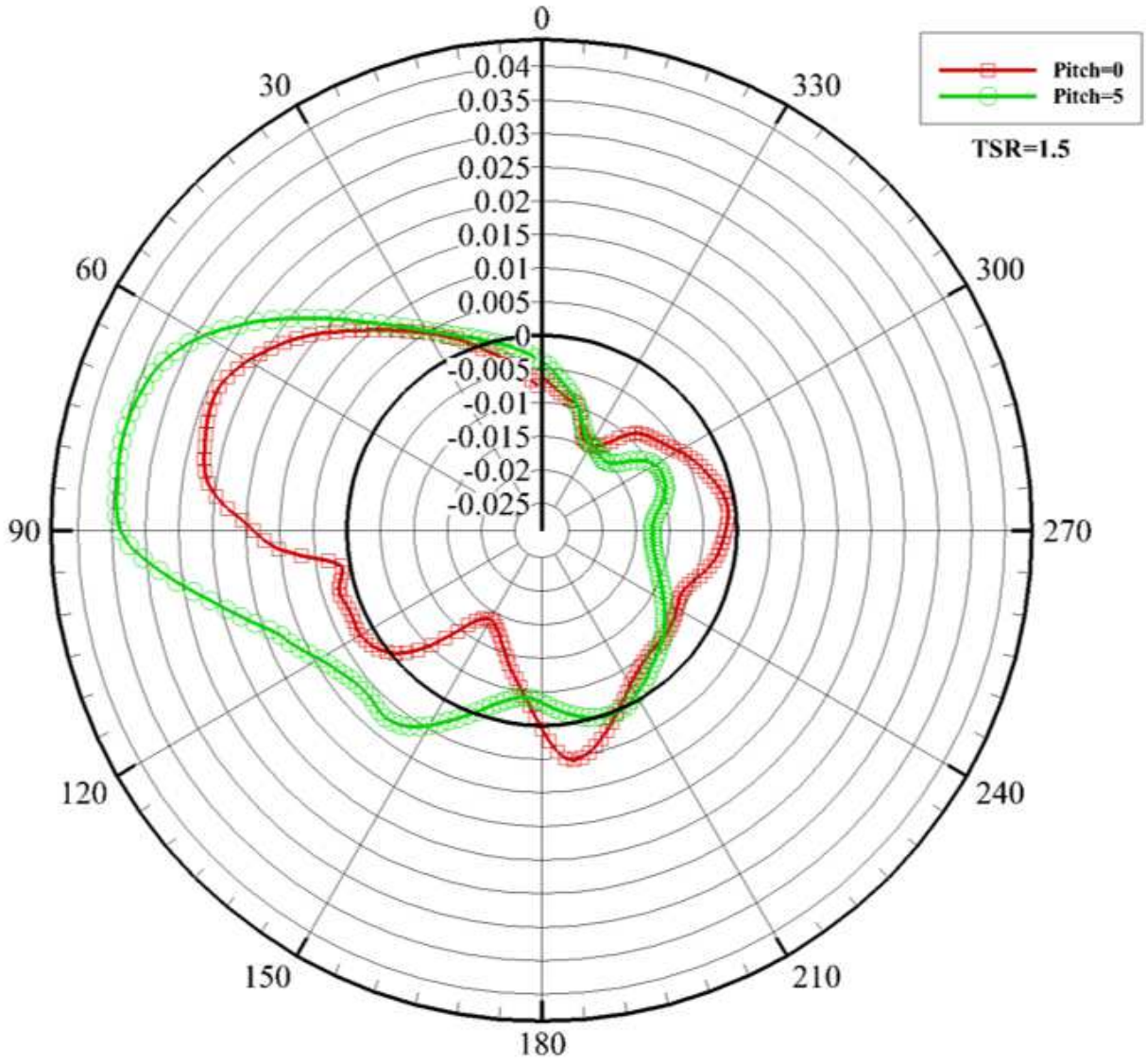

Figure 10

Evolution of CT as function of Azimuth position for a single blade at TSR=1.5; pitch=0(red) and pitch=5(green)

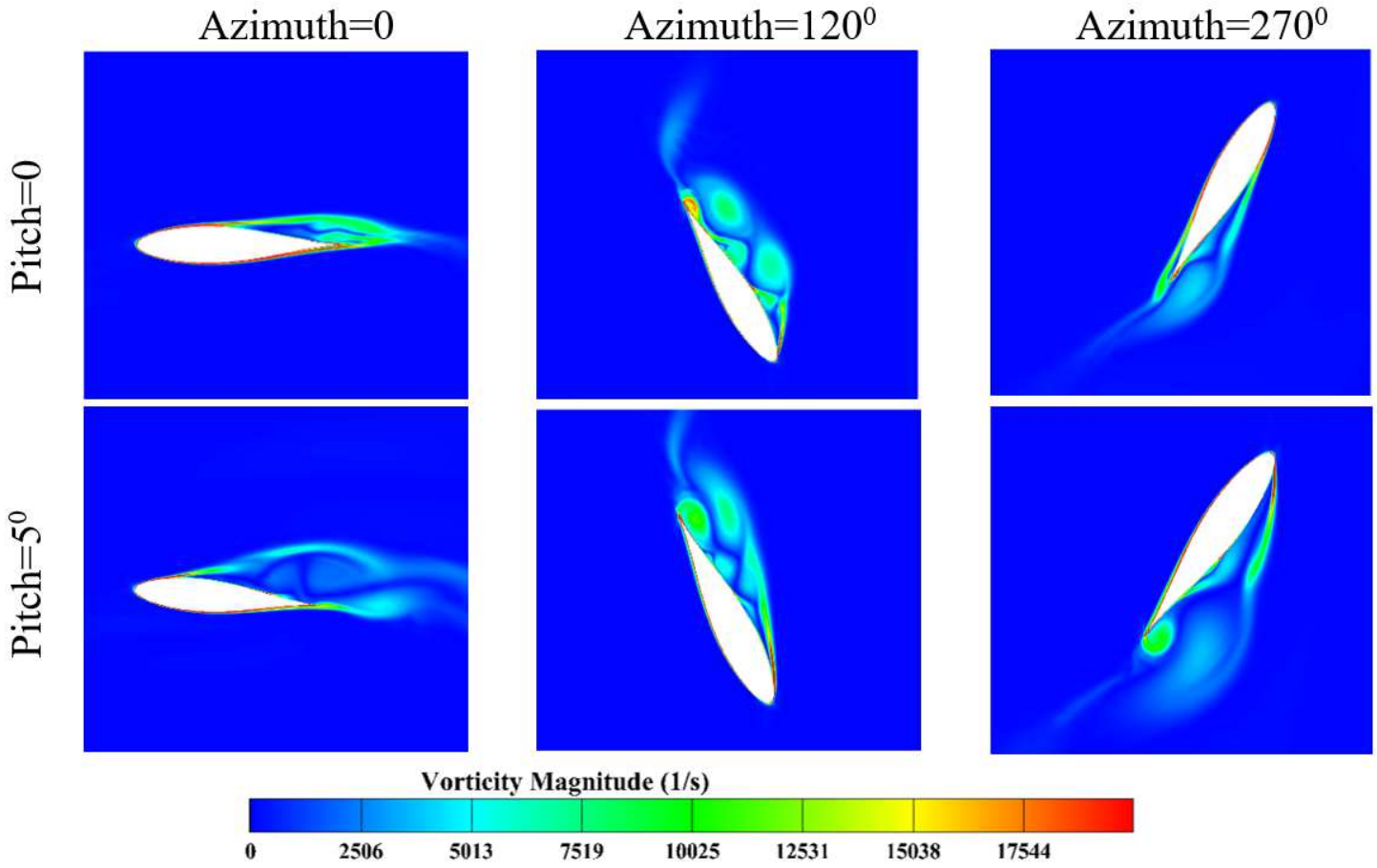

Figure 11

Vorticity magnitude (1/s); TSR=2

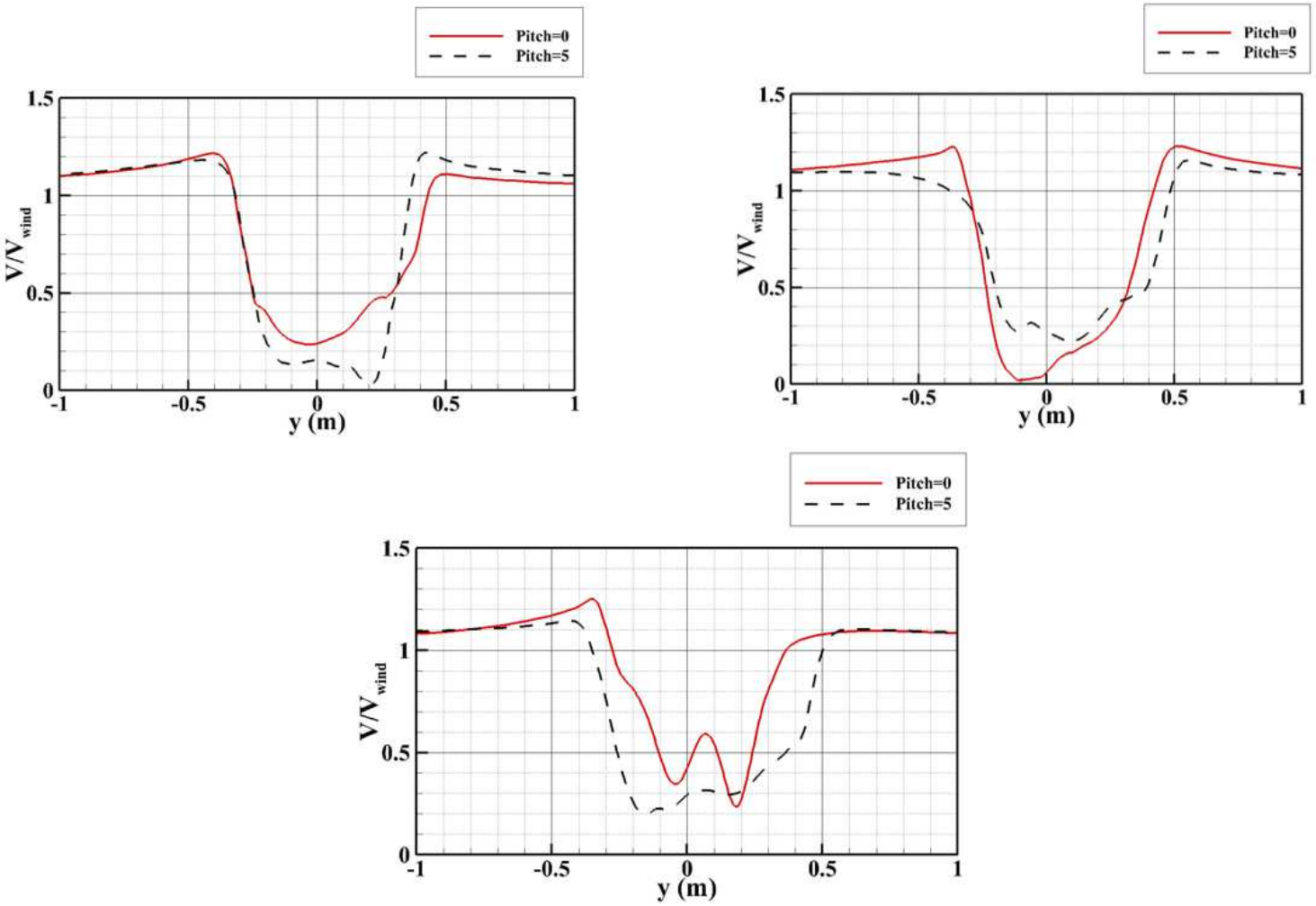

Figure 12

Cross stream dimensionless velocity profile in 1D, 2D and 3D lateral distance of turbine (CFD results)